International Journal of Nanomedicine

Dovepress
open access to scientific and medical research

Open Access Full Text Article

ORIGINAL RESEARCH

Hair Follicle-Targeted Delivery of Azelaic Acid Micro/Nanocrystals Promote the Treatment of Acne Vulgaris

Yan Ji[1], Haorong Li[1], Jiguo Li[2], Guangqiang Yang[1], Wenli Zhang[1], Yan Shen[1], Bohui Xu[3], Jianping Liu[1], Jingyuan Wen[4], Wenting Song[1]

[1]Department of Pharmaceutics, School of Pharmacy, China Pharmaceutical University, Nanjing, People's Republic of China; [2]Nanjing Miaobang Meiye Enterprise Management Co, LTD, Nanjing, People's Republic of China; [3]School of Pharmacy, Nantong University, Nantong, 226001, People's Republic of China; [4]School of Pharmacy, Faculty of Medical and Health Sciences, the University of Auckland, Auckland, New Zealand

Correspondence: Wenting Song, Department of Pharmaceutics, School of Pharmacy, China Pharmaceutical University, 639 Longmian Avenue, Jiangning District, Nanjing, 211198, People's Republic of China, Email songwenting908@163.com; Jingyuan Wen, School of Pharmacy, Faculty of Medical and Health Sciences, the University of Auckland, Auckland, New Zealand, Email j.wen@auckland.ac.nz

Purpose: Acne vulgaris is a chronic inflammatory skin disorder centered on hair follicles, making hair follicle-targeted delivery of anti-acne drugs a promising option for acne treatment. However, current researches have only focused on the delivering to healthy hair follicles, which are intrinsically different from pathologically clogged hair follicles in acne vulgaris.

Patients and Methods: Azelaic acid (AZA) micro/nanocrystals with different particle sizes were prepared by wet media milling or high-pressure homogenization. An experiment on AZA micro/nanocrystals delivering to healthy hair follicles was carried out, with and without the use of physical enhancement techniques. More importantly, it innovatively designed an experiment, which could reveal the ability of AZA micro/nanocrystals to penetrate the constructed clogged hair follicles. The anti-inflammatory and antibacterial effects of AZA micro/nanocrystals were evaluated in vitro using a RAW264.7 cell model stimulated by lipopolysaccharide and a Cutibacterium acnes model. Finally, both the anti-acne effects and skin safety of AZA micro/nanocrystals and commercial products were compared in vivo.

Results: In comparison to commercial products, 200 nm and 500 nm AZA micro/nanocrystals exhibited an increased capacity to target hair follicles. In the combination group of AZA micro/nanocrystals and ultrasound, the ability to penetrate hair follicles was further remarkably enhanced (*ER* value up to 9.6). However, toward the clogged hair follicles, AZA micro/nanocrystals cannot easily penetrate into by themselves. Only with the help of 1% salicylic acid, AZA micro/nanocrystals had a great potential to penetrate clogged hair follicle. It was also shown that AZA micro/nanocrystals had anti-inflammatory and antibacterial effects by inhibiting pro-inflammatory factors and Cutibacterium acnes. Compared with commercial products, the combination of AZA micro/nanocrystals and ultrasound exhibited an obvious advantage in both skin safety and in vivo anti-acne therapeutic efficacy.

Conclusion: Hair follicle-targeted delivery of AZA micro/nanocrystals provided a satisfactory alternative in promoting the treatment of acne vulgaris.

Keywords: acne vulgaris, azelaic acid, hair follicle, micro/nanocrystals, targeted delivery

Introduction

Acne vulgaris ranks 8th in prevalence among diseases and 2nd in the list of global skin diseases.[1] Acne vulgaris is a common skin disease, affecting millions of people of different ages and severities around the world.[2] Its manifestations can appear in waves, with the mild form including comedonal acne and papulopustular acne, the moderate form including papulopustular acne and nodular acne, and the severe form including nodulocystic acne and conglobate acne.[3] If acne is not treated appropriately, it may leave permanent scars, and improper treatment can also cause serious secondary infections, damaging the normal function of the skin.[4] Acne patients may experience dissatisfaction with their appearance and a decline in overall quality of life, negatively impacting their personal, social life, and mental health.[5,6]

Received: 15 January 2024
Accepted: 28 May 2024
Published: 4 June 2024

Currently, recommended topical anti-acne drugs include antibiotics and anti-inflammatory agents such as adapalene, clindamycin, benzoyl peroxide, retinoid tretinoin and azelaic acid.[7] Although these drugs have certain anti-acne therapeutic effects, they often cause obvious skin irritation and adverse reactions such as skin dryness, desquamation, erythema and tingling.[8,9] In an attempt to decrease skin adverse reactions, some commercial products contain these drugs in very small amounts, resulting in limited therapeutic effects.[10] Other commercial products increase the amount of these drugs to achieve a better anti-acne effect, but this inevitably worsens skin adverse reactions.[11] In summary, these anti-acne drugs have not achieved a balance between anti-acne efficacy and skin safety, leading to delayed effective treatment and the aggravation of acne.

Acne vulgaris is a chronic inflammatory skin disorder centered on the hair follicle.[12] Altered sebum production and follicular hyperkeratinization lead to the clogging of hair follicles, resulting in the overgrowth of Cutibacterium acnes and increased inflammation in hair follicles.[12,13] Consequently, the key target for acne treatment is the hair follicle rather than the well-known stratum corneum.[14] From this perspective, it is crucial to determine whether anti-acne drugs can be delivered efficiently to hair follicles. Most anti-acne drugs weaken the stratum corneum barrier. If these drugs penetrate into the stratum corneum, they can destroy the skin barrier and cause further irritation in the deeper epidermis.[15] Therefore, hair follicle-targeted delivery of anti-acne drugs, increasing drug distribution to hair follicles without enhancing penetration into the stratum corneum, is of major interest in acne treatment. This may improve the therapeutic efficacy of anti-acne drugs and reduce the incidence and severity of adverse skin reactions.[16]

Recent reports have demonstrated that nanoparticles can localize to hair follicles, including polymer nanoparticles,[17] lipid nanoparticles,[18,19] metal nanoparticles,[20,21] nanostructured lipid carriers,[22,23] and micro/nanocrystals.[24,25] Several factors of nanoparticles determine the ability of hair follicle-targeted delivery, such as particle size,[26] lipophilicity,[27] particle shape[28] and surface charge,[29] among others. Especially, particle size was reported to have a significant influence on the targeted behavior of nanoparticles to hair follicles.[28] Although some studies suggest the hair follicle-targeted delivery could improve the anti-acne effect,[30] several important issues still remain unknown: (1) Compared with healthy hair follicles, the hair follicles that develop acne undergo obvious changes in morphology, clogged at the infundibulum level by a plug formed by keratinocytes.[2] Consequently, anti-acne drugs need to be delivered into clogged hair follicles rather than healthy ones to improve actual anti-acne efficacy. Existing research has only focused on delivery to healthy hair follicles,[31,32] providing misleading information for guiding the improvement of anti-acne efficacy. (2) There is a lack of anti-acne efficacy evaluation in vitro and in vivo to clarify whether hair-follicle targeted delivery has an advantage over existing commercial products in improving therapeutic outcomes.[33,34] The absence of anti-acne efficacy feedback significantly hinders further optimization and application of hair follicle-targeted delivery in acne treatment.

In this study, azelaic acid (AZA) micro/nanocrystals of different particle sizes were prepared. Hair follicle-targeting experiments were performed to compare the hair follicle-targeting ability of different AZA micro/nanocrystals and commercial products containing AZA in a dissolved state in healthy skin. More importantly, an innovative experiment on targeted delivery to clogged hair follicles was introduced using a constructed skin model with clogged hair follicles. Based on this model, the penetrating ability of AZA micro/nanocrystals to clogged hair follicles was further optimized. Then, an experiment with anti-inflammatory RAW 264.7 macrophages experiment and a Cutibacterium acnes inhibition experiment were conducted to evaluate the anti-acne effect of AZA micro/nanocrystals in vitro. Finally, the in vivo anti-acne effects and skin safety of AZA micro/nanocrystals and commercial products were compared.

Materials and Methods

Materials

AZA was purchased from Brillian Co. Ltd. (Beijing, China). Lactobacillus ferment and Piper methysticum extract were purchased from Setic Co. Ltd. (Guangzhou, China). Fluoro-max was purchased from Thermo Fisher Scientific Co. Ltd. (Shanghai, China). Tween 80 and dexamethasone were obtained from Sinopharm Chemical Reagent Co. Ltd. (Nanjing, China). Salicylic acid was purchased from Belrice Biotechnology Co., Ltd. (Beijing, China) and was encapsulated in hydroxypropyl cyclodextrin. Lipopolysaccharide (LPS) was obtained from Yuanye Bio-Technology Co., Ltd. (Shanghai,

China), and plant extracts were purchased from Nutri-Woods Bio-tech Co., Ltd. (Beijing, China). All other chemicals and reagents were obtained from Aladdin Co. Ltd. (Shanghai, China).

Cell Lines and Animals

RAW 264.7 macrophages were obtained from KeyGen Biotech Co. Ltd. (Nanjing, China). New Zealand white rabbits (2.5 kg±0.5 kg) were obtained from Qing Longshan Animal Co., Ltd. (Nanjing, China) and were fed at 25 °C and 55% humidity under natural light/dark cycles. All experimental procedures were performed according to protocols approved by the Animal Care and Use Committee of China Pharmaceutical University. The ethical and legal approval code is 2023-03-019, which is approved by Medical Ethics Committee of China Pharmaceutical University.

Preparation and Characterization of AZA Micro/Nanocrystals

Preparation of AZA Micro/Nanocrystal Suspensions

As listed in Table 1, different AZA micro/nanocrystal suspensions were prepared with the same composition and an acceptable minimum amount of Tween 80 as the stabilizing agent. Micro/nanocrystals with different particle sizes were prepared by the high-pressure homogenization method or wet media milling method,[35] respectively. Micro/nanocrystal suspensions of 500 nm, 1000 nm, and 1500 nm were prepared by the high-pressure homogenization method: First, AZA powder was dispersed at a speed of 10,000 rpm for 9 min to obtain coarse suspensions. This was followed by high-pressure homogenization, as shown in Table 1. 200 nm micro/nanocrystals were prepared by the wet media milling method: First, AZA powder was dispersed in Tween 80 solution with sonication for 10 min. The formed suspensions and 0.2 mm zirconium oxide beads were then added (2:1, v/v) to a glass vial and ground for 24 h at a speed of 400 rpm.

Preparation of AZA Micro/Nanocrystal Freeze-Dried Powder

The micro/nanocrystal suspensions were freeze-dried to ensure the stability of the formulation and maintain the particle size of the AZA micro/nanocrystals. As a freeze-drying protectant, trehalose was added to the micro/nanocrystal suspensions at a ratio of 1:20 (w/v) prior to freeze-drying. Subsequently, the micro/nanocrystal suspensions were placed in a freeze-dryer with the experimental parameters set at −40 °C and 20 Pa for 48 h after pre-freezing in a −80 °C refrigerator. The freeze-dried powder was re-dispersed in distilled water in the following steps. The freeze-dried powder was added to distilled water at a ratio of 1:10 (w/w) and shaken well until there were no obvious particles. The particle sizes of the AZA micro/nanocrystals were measured before and after freeze-drying operation.

Characterization of AZA Micro/Nanocrystals

The average particle size and polydispersity index (PDI) of the micro/nanocrystal suspensions and freeze-dried powder were measured using a particle size potentiometer (Brookhaven, USA). The measurement temperature was 25 °C. Each sample was analyzed three times. The surface structure and morphology of the micro/nanocrystals were analyzed by scanning electron microscopy (SEM). Samples of different particle sizes were analyzed at a magnification of 5000x. The intensities of X-ray diffractions of AZA raw material powder and AZA micro/nanocrystal freeze-dried powder were measured between 4–40° 2θ.

Table 1 Prescription Composition and Preparation Method of AZA Micro/Nanocrystals with Different Particle Sizes

Particle Size	Prescription Composition		Preparation Method
	AZA (% w/v)	Tween 80 (% w/v)	
200 nm	5	0.1	400 rpm for 24 h
500 nm	5	0.1	1200 bar for 10 min
1000 nm	5	0.1	1000 bar for 5 min
1500 nm	5	0.1	800 bar for 5 min

Experiment of Targeting Hair Follicles in Healthy Skin

In vitro Skin Penetration Study

The rabbits were sacrificed, the inner skin of the outer ear was excised, and the subcutaneous fat was removed. The skin was fixed on Franz cells at an experimental temperature of 32 °C and stirring speed of 400 rpm. The receptor compartment was filled with 0.9% NaCl solution and 300 μL of the different preparations was added to the donor cell, which included AZA coarse suspensions, AZA micro/nanocrystals with different particle sizes and commercial products. Also, the combination groups of micro/nanocrystals and ultrasound operation, micro/nanocrystals and radio-frequency operation, and micro/nanocrystals and ultrasound operation with 1% salicylic acid were set up. After 45 min of skin penetration in combination groups, an ultrasound transducer (20 kHz, 1.15 w/cm^2) or a radiofrequency transducer (1.5 MHz) was immersed in the donor fluid of Franz cells and placed at the skin surface (avoid overheating) for 15 min at room temperature. At 1 h, the residual preparations on the skin surface were washed with a quantitative receiver solution and skin samples were obtained for subsequent experiments.

Sample Preparation of Stratum Corneum, Hair Follicle and Remaining Layers

The rabbit skin obtained in the above experiment of "In vitro skin penetration study" was further treated to get the samples of stratum corneum, hair follicle and remaining layers using the tape stripping method. The first two tapes were discarded to avoid overestimating the amount of AZA in stratum corneum. The stratum corneum sample was obtained by tape stripping for the next 12 times at the penetration area in skin penetration study.[36] Hair follicle samples were collected following the removal of stratum corneum from the skin sample.[37] A drop of cyanoacrylate was applied to the penetration area, followed by the covering with a tape. After 5 min, a hair follicle sample was obtained by removing the tape with quick movement.[38,39] The remaining skin was shredded with scissors into pieces to obtain a sample of the remaining layers. All samples were then added to ethanol (2.5 mL) and extracted using ultrasound for 30 min. The amount of AZA in the resulting aliquots was quantitatively analyzed.

Quantitative Analysis of AZA Amount

AZA was first derivatized into AZA esters for further quantitative analysis.[40] To the collected sample solution, 2 mL of ethanol and 800 μL of concentrated sulfuric acid were added and incubated at room temperature for 10 min to obtain the derivatized solution. Subsequently, 5 mL n-hexane was added to the derivatized solution, followed by vertexing for 1 min and centrifugation for 5 min (≥ 5000 rpm). After two repeated extractions, the extract was washed with 15 mL saturated $NaHCO_3$ solution and centrifuged for 5 min (≥ 5000 rpm). After the n-hexane layer was blown off using nitrogen, the volume was adjusted to 0.5 mL with n-hexane, resulting in the test sample solution.

The AZA content in the stratum corneum and hair follicle samples was analyzed by gas chromatography using an HP-5 chromatographic column (30 m × 0.25 mm × 0.25 μm). The effluent was split in a ratio of 5:1. Hydrogen gas was used as the carrier gas (a flow rate of 30 mL/min). The following oven temperature program was used: an initial column temperature of 80 °C was held for 2 min, then the temperature was increased to 250 °C at a rate of 20 °C/min, and held at 250 °C for 6 min. The detector temperature was set at 280 °C. The method was linear in the concentration range 3–50 μg/mL. The limit of quantification (LOQ) of the assay was validated at 0.27 μg/mL.

The enhancement ratio (*ER*) of penetrating hair follicles was calculated to evaluate the hair follicle-targeting ability of different AZA formulations, as illustrated in Equation 1.

$$ER=C_x/C_1 \quad (1)$$

Where C_χ is the AZA content in the hair follicles in the experimental group and C_1 is the AZA content in the hair follicles in the commercial product group. A higher *ER* value indicates a strong ability to penetrate hair follicles.

Experiment of Penetrating into Clogged Hair Follicles

Construction of Acne Skin Model with Clogged Hair Follicles

2.3–2.5 kg New Zealand white rabbits were selected. 200 μL mixture of liquid paraffin and oleic acid (1:1, v/v) was topically applied to a 2 cm × 2 cm area on the inner side of the skin of the outer ear once a day. After approximately 10

days, an acne-skin model with clogged hair follicles was established. The morphology and histology of the clogged hair follicles were characterized by dermatoscopic observation and oil red O staining.

Pretreatment of Acne Skin Model

The acne skin model with clogged hair follicles was fixed on Franz cells under the same experimental conditions described in Section *2.4.1*. Different test formulations (300 μL) were added to the donor cells: AZA micro/nanocrystals, Lactobacillus ferment, 0.1% salicylic acid, and 1% salicylic acid. Saline solution was added to the donor cells as a control group. After 1 h, the residual formulations on the skin surface were washed with quantitative receiver solution. Subsequently, all skin surfaces of the penetration area were covered with six layers of cyanoacrylate, except for the acne area where the hair follicles were clogged.

Confocal Laser Scanning Microscopy (CLSM)

Because AZA micro/nanocrystals do not possess fluorescent characteristics, fluorescent microspheres with a particle size of 1000 nm were employed as substitutes for AZA micro/nanocrystals to investigate their penetration into hair follicles. First, pretreated skin samples were fixed to Franz cells. Next, 300 μL of the fluorescent microsphere suspension was added to the donor cell. The other conditions were the same as described in Section 2.4.1 (In vitro skin penetration study). After 1 h, the skin samples were removed and observed using CLSM. A wavelength of 555 nm was selected for fluorescence excitation. The fluorescent signal was detected at a wavelength of 585 nm. Digital images were obtained, and penetration depths were measured using the Zen®Soft software.

Anti-Inflammatory Experiment in LPS Treated Macrophages

Cell Culture and Viability

RAW 264.7 macrophages were cultured in Dulbecco modified Eagle medium with 10% fetal bovine serum, 1% penicillin, and 1% streptomycin. The cells were cultured in a humid environment containing 5% carbon dioxide at 37 °C. Subculturing was performed every two days.

The cell viability was detected by MTT (3-methylazolyl-5-methyl-thiazolyl-2-5-diphenyltetrazolium) colorimetric method. The tested groups were AZA micro/nanocrystals, Piper methysticum extract, Dendrobium candidum extract, and A. barbadensis extract at concentrations of 0.1, 0.2, 0.3, 0.4, and 0.5% (w/v). The absorbance was measured using a microplate reader at 570 nm. This method measures succinate dehydrogenase activity at the mitochondrial level, which is an indicator of cell viability. The safe concentration of each solution was evaluated based on the normal growth of cells.

Determination of Inflammatory Factors

RAW 264.7 macrophages (5×10^4 cells/well) were seeded in 96-well plates. After 24 h, a 0.2% drug solution diluted with the culture medium was added. Two hours later, 5 μg/mL LPS was added to stimulate the cells to produce an inflammatory reaction.[41] After incubation for 24 h, the supernatant was collected by centrifugation at 1000 rpm for 10 min. The levels of IL-6 and TNF-α were determined using an ELISA kit, according to the manufacturer's protocol.

Antibacterial Experiment in Cutibacterium Acnes

Culture of Cutibacterium Acnes

Cutibacterium acnes (ATCC® 11827TM) was cultured in liquid thioglycolate medium. Frozen bacteria (100 μL) were inoculated into the culture medium, sealed in a culture box containing anaerobic gas-producing bags, and cultured on a shaker at 37 °C for 96 h.[42]

Antibacterial Experiment on Cutibacterium Acnes

Potential antibacterial solutions at concentrations of 0.05, 0.1, 0.15, 0.2, and 0.25% (w/v) were placed in a 96-well plate in a culture box for deoxygenation using anaerobic gas-producing bags. The Cutibacterium acnes was diluted with saline solution to adjust the concentration, and the absorbance was measured using an ultraviolet spectrophotometer. The target concentration was obtained when the absorbance reached 0.1, and was further diluted by 10 times. Ten microliters of diluted Cutibacterium acnes solution was inoculated in the aforementioned 96-well plate

and cultured at 37 °C for 72 h. MIC was defined as the minimum concentration of antibacterial solutions inhibiting visible growth of Cutibacterium acnes.[42] The inhibition rate of different antibacterial solutions on Cutibacterium acnes was evaluated by measuring the absorbance at 600 nm with a microplate reader, as calculated in Equation 2.

Inhibition rate= (1–1/n) x100% (2)

I: absorbance of the test group solution; *II*: absorbance of the control group solution.

Skin Irritation Test

The skin irritation test was carried out on the abdominal skin of New Zealand white rabbits to evaluate the skin irritation of AZA micro/nanocrystal and AZA commercial products, with five rabbits per group.[43] Group A was treated with blank solvent (negative control), group B was treated with 5% sodium dodecyl sulfate solution (positive control), group C was treated with 10% 500 nm AZA micro/nanocrystals containing 1% salicylic acid combined with 1.15 w/cm^2 ultrasound for 5 min, group D was treated with 10% AZA commercial products. After 2 h of application, skin irritation was evaluated according to visual erythema as follows: no erythema, 0; mild erythema (light pink), 1; moderate erythema (deep pink), 2; moderate to severe erythema (light red), 3; and severe erythema (extreme redness), 4. Higher scores indicated stronger skin irritation.

In vivo Evaluation of Therapeutic Effect on Acne

Construction and Characterization of Composite Acne Model

One hundred microliters of inactivated Cutibacterium acnes solution (1 × 10^7 CFU/mL) was intradermally injected at four sites in a 2×2 cm area on the inner skin of the outer ear of the experimental rabbits. This was followed by topical application of 200 μL 30% oleic acid in liquid paraffin once a day for 14 days. The composite acne model was characterized by dermatoscopic and histological analyses.

Treatment Regimen

Three groups were set up for treatment once a day for 4 consecutive days: (1) no treatment (control group); (2) 300 μL 10% 500 nm AZA micro/nanocrystals containing 1% salicylic acid combined with ultrasound for 5 min at an intensity of 1.15 w/cm^2 (experimental group); (3) 300 μL of a commercial product gel containing 10% AZA (commercial group), with five rabbits per group.

Evaluation of Anti-Acne Therapeutic Effect

Changes in hair follicles at the model construction and treatment stages were observed using a digital camera and dermatoscope for a clearer vision and quantitative description of acne morphology. Changes in acne diameter and color differences between the acne area and the surrounding skin area were calculated. The skin tissue was fixed in 4% paraformaldehyde for 48 h and then divided into two parts for histological analysis: one part was embedded in paraffin and stained with H&E, and the other part was embedded with an OTC embedding agent and stained with Oil Red O. All slices were 5 μm thick. Pathological changes in the ear tissue and accumulation of inflammatory cells were observed under a microscope after H&E staining. Changes in the sebaceous glands were observed under a microscope after oil red O staining.

Statistical Analysis

The data obtained from the experiments were expressed as the mean ± SD (standard deviation) and representative of three or four independent experiments with the exception of the data in "skin irritation test" and "In vivo evaluation of therapeutic effect on acne". In each independent experiment, two technical replicates are conducted. A one-way analysis of variance (ANOVA) with the Bonferroni correction was used to determine significant differences, and the level was set at $p < 0.05$ (*), $p < 0.01$ (**), $p < 0.001$ (***), and $p < 0.0001$ (****).

Results and Discussion

Characterization of AZA Micro/Nanocrystal Suspensions

A photograph of the AZA micro/nanocrystal suspension is shown in Figure 1A. In Table 2, the particle sizes of the four different AZA micro/nanocrystal suspensions are analyzed at both 0 h and 24 h after preparation. It revealed that the required micro/nanocrystals particle size of 200 nm, 500 nm, 1000 nm and 1500 nm were achieved with relatively narrow size distribution (PDI from 0.16 to 0.32), respectively. The particle distribution of AZA micro/nanocrystals and coarse suspensions was illustrated in Supplement Figure 1. Additionally, the particle size remained unchanged after 24 h of preparation.

Characterization of AZA Micro/Nanocrystal Freeze-Dried Powder

A photograph of the freeze-dried AZA micro/nanocrystal powder is shown in Figure 1B. As shown in Figure 1C, compared with the AZA micro/nanocrystal suspensions before freeze-drying, the particle size of the AZA micro/nanocrystals after the redispersion of the freeze-dried powder did not significantly change. The morphology of the AZA micro/nanocrystals was characterized by scanning electron microscopy (SEM). SEM images of the AZA micro/nanocrystals are shown in Figure 1D-G, respectively. The AZA micro/nanocrystals possessed a cubic shape, and the average sizes of the AZA micro/nanocrystals were 200, 500, 1000, and 1500 nm, respectively, showing particle sizes similar to those measured by DLS. As illustrated in powder X-ray diffraction diffractograms (Supplement Figure 2), the peak position of 500 nm AZA micro/nanocrystal freeze-dried powder with or without trehalose overlapped with AZA raw material powder, which suggested the crystal form remained unchanged.

Hair Follicle-Targeted Delivery of AZA Micro/Nanocrystals in Healthy Skin

To reveal the hair follicle-targeting behavior of the AZA micro/nanocrystals, groups were established for the commercial product and coarse suspensions, each containing the same AZA concentration as the AZA micro/nanocrystal groups. Surprisingly, in comparison to these two groups, the amount of AZA in the hair follicles in the micro/nanocrystal groups of 200 nm and 500 nm was significantly increased, but the amount in the stratum corneum did not show a clear increase (Figure 2A). AZA was not detected in the remaining skin samples from any group. Among all micro/nanocrystal groups, the group with 500 nm micro/nanocrystals exhibited the highest ability to penetrate hair follicles, with an *ER* value of 3.8 (Figure 2B). Unexpectedly, in the micro/nanocrystal and ultrasound combination group with or without 1% salicylic acid, the ability to penetrate hair follicles was remarkably enhanced (*ER* value up to 9.6 and 7.7) (Figure 2B), which was consistent with previous reports indicating that particles with optimal sizes in the range of 400–700 nm tended to accumulate preferentially within the hair follicles.[44] This may be explained that low-frequency ultrasound induces inertial cavitation bubbles, whose collapse leads to high-speed microjets directed toward the skin surface and shock-waves, causing the enhancement of AZA micro/nanocrystals penetration into the follicles.[45] Differently, the combination of micro/nanocrystal and radiofrequency did not show remarkable influence on the penetrating ability into hair follicles (*ER* = 1.5) (Figure 2B).

Penetration of AZA Micro/Nanocrystals into Clogged Hair Follicles

Characterization of Acne Skin Model with Clogged Hair Follicles

Compared to healthy hair follicles, hair follicles that developed acne exhibited obvious changes in morphology. The hair follicles were significantly dilated and obstructed at the infundibulum level by a plug formed by sebum and keratinous material shed from the skin.[46] Therefore, it was crucial to investigate whether micro/nanocrystals could penetrate the clogged hair follicles rather than only healthy ones, which, unfortunately, were limited.[44,47] In this study, an acne model with clogged hair follicles was constructed and characterized. Compared with healthy hair follicles, there were obvious red lesions in the constructed acne skin model (Figure 3A and D), and the hair follicles were clogged with significant expansion (Figure 3B and E). As demonstrated in oil red O staining observation of tissue slices (Figure 3C and F), there was obvious hyperkeratinization in the part of infundibulum of hair follicles, clogged by keratinous material and lipid substances stained orange. The above characterization results indicated that an acne skin model with clogged hair follicles was established.

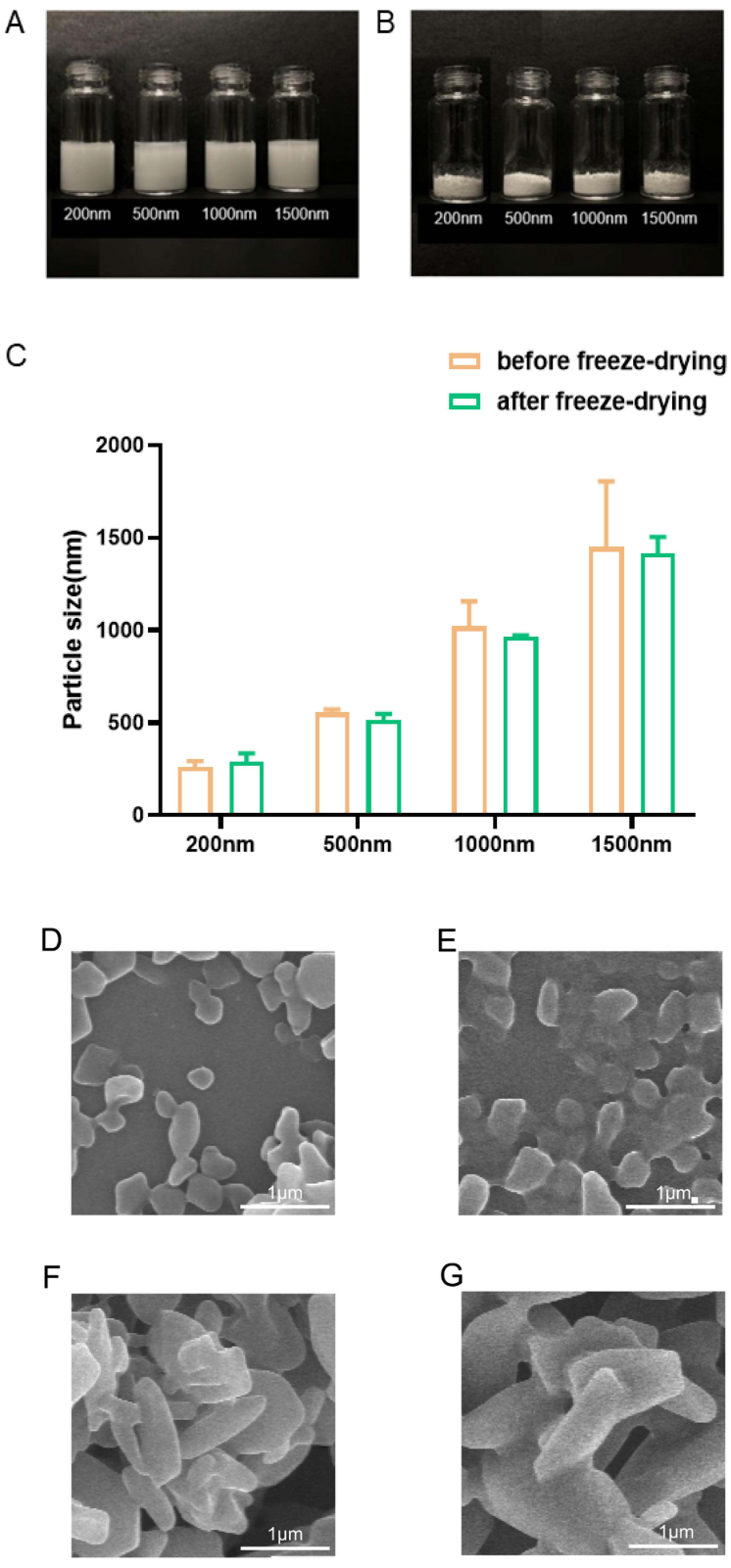

Figure 1 The morphology of AZA micro/nanocrystal suspensions (**A**) and AZA micro/nanocrystal freeze-dried powder (**B**). (**C**) Particle size of AZA micro/nanocrystals before and after freeze-drying (n=3, mean ±SD). SEM micrograph of 200 nm (**D**), 500 nm (**E**), 1000 nm (**F**) and 1500 nm (**G**).

Table 2 Particle Size and PDI (Polydispersity Index) of AZA Micro/Nanocrystal Suspensions (n=3, mean±SD)

Required Size	0 h		24 h	
	Particle Size/nm	PDI	Particle Size/nm	PDI
200 nm	246.33 ± 21.73	0.32 ± 0.05	254.11 ± 39.23	0.32 ± 0.05
500 nm	499.88 ± 72.03	0.25 ± 0.02	554.51 ± 101.33	0.21 ± 0.07
1000 nm	1052.70 ± 35.23	0.27 ± 0.04	1065.76 ± 42.09	0.24 ± 0.03
1500 nm	1451.69 ± 67.34	0.26 ± 0.03	1486.72 ± 44.33	0.16 ± 0.04

Improved Penetration Ability of AZA Micro/Nanocrystals in Presence of Salicylic Acid

Owing to the absence of existing research methods for evaluating the ability of particles to penetrate clogged hair follicles, the design of this study was initiated. A schematic of the experimental design is shown in Figure 4. Considering the difficulty in obtaining clogged hair follicle samples for quantitative analysis, CLSM was employed to illustrate the penetrating ability of AZA micro/nanocrystals into the clogged hair follicles. Patzelt et al reported that the penetrating ability of particles to hair follicles was more likely to be determined by a mechanical effect related to particle size rather than an effect specific to particles.[48] Therefore, because of the absence of the fluorescent property of AZA, fluorescent microspheres (1000 nm) were employed as a substitute for AZA micro/nanocrystals with a particle size of 1000 nm for CLSM observation. Apart from the clogged hair follicles, all other skin surfaces were covered with six layers of cyanoacrylate, through which fluorescent microspheres could not penetrate.[49,50] Notably, the skin model was pretreated with different solutions using Franz cells to investigate their potential to open the clogged hair follicles and thus help fluorescent microspheres penetrate the hair follicles. In the control group, saline solution was used to pretreat the skin model. As shown in Figure 5, the circled area represents the position of the clogged hair follicle on the skin surface, which is the only area free from covering the cyanoacrylate layers. There was no obvious fluorescence intensity in the control group from the skin surface to the 30 μm depth of the skin layer. This proved that the cyanoacrylate layers could prevent the fluorescent microspheres from penetrating the covered skin. This demonstrates that the fluorescent microspheres themselves could not penetrate the clogged hair follicles.

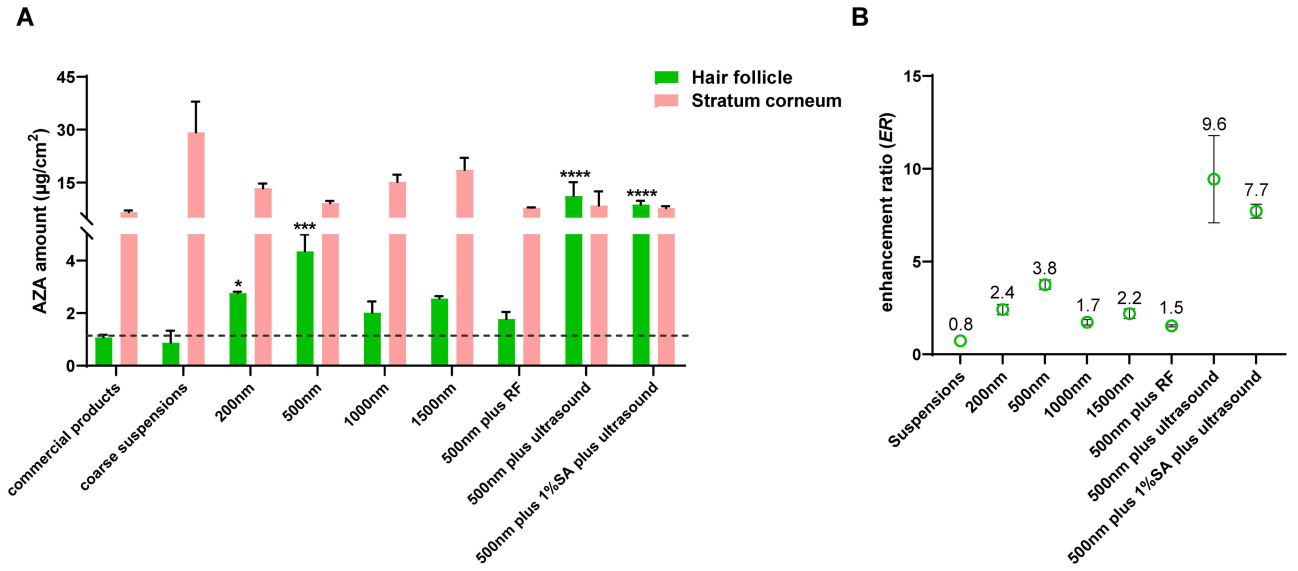

Figure 2 (**A**) The amount of AZA in stratum corneum and hair follicle. (**B**) The enhancement ratio (ER) of penetrating hair follicles in comparison to commercial product, *p < 0.05, ***p < 0.001, ****p < 0.0001 (n=4, mean ± SD).
Abbreviations: RF, radiofrequency operation; SA, salicylic acid.

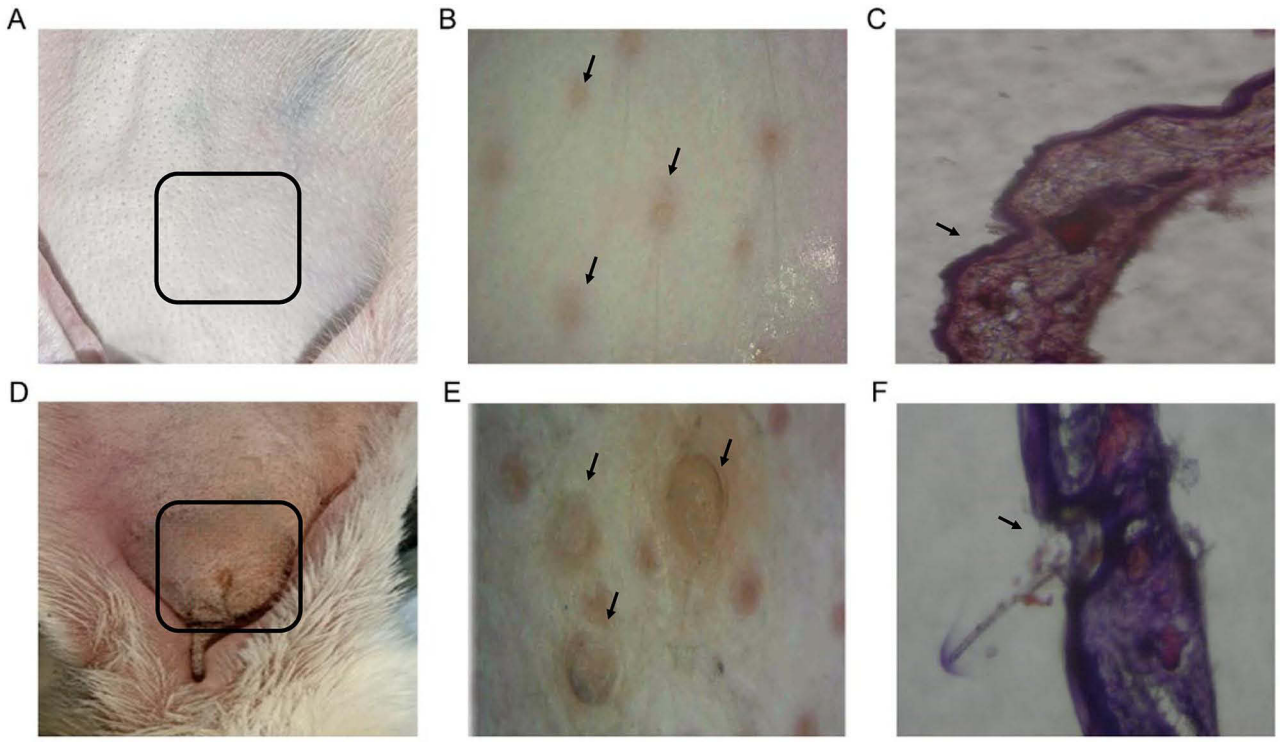

Figure 3 (**A**) Visual observation of hair follicles in healthy skin, (**B**) Dermatoscope observation of hair follicles in healthy skin, (**C**) Oil red O staining observation of hair follicles in healthy skin, (**D**) Visual observation of clogged hair follicles in acne skin model, (**E**) Dermatoscope observation of clogged hair follicles in acne skin model, (**F**) Oil red O staining observation of clogged hair follicles in acne skin model. The squircles indicate the position of constructing acne skin model. The black arrows indicate the position of hair follicles.

Based on the above analysis of the results in the control group, it was safe to conclude that the fluorescence intensity in Figure 5 represented the ability of the fluorescence microspheres to penetrate clogged hair follicles. In the AZA micro/nanocrystal group, AZA micro/nanocrystals with a particle size of 1000 nm were employed as a representative of AZA micro/nanocrystals to pretreat the skin model. Thus, the potential of opening clogged hair follicles and helping fluorescent microspheres penetrate hair follicles was evaluated. As illustrated in Figure 5, only a very weak fluorescence intensity was detected in the AZA micro/nanocrystal group, indicating that AZA micro/nanocrystals cannot easily penetrate the clogged hair follicles by themselves. The order of fluorescence intensity in the other test groups was as follows: 1% salicylic acid > 0.1% salicylic acid > Lactobacillus fermentation filtrate. All groups exhibited improved penetration into clogged hair follicles. Among these, the 1% salicylic acid group showed the strongest fluorescence intensity. This was because that salicylic acid was an excellent keratolytic agent, which may reduce corneocyte adhesion in the position of hyperkeratinization in the clogged hair follicles.[51] From this point, only with the help of 1% salicylic acid, AZA micro/nanocrystals had a great potential of penetrating into the clogged hair follicle. Therefore, the composition of the AZA micro/nanocrystals was further optimized using 1% salicylic acid. It was worth noting that although AZA was also reported to have keratolytic activity,[52] it was not strong enough to open the clogged hair follicles and help AZA micro/nanocrystals penetrate them.

In vitro Anti-Inflammatory Effect of AZA Micro/Nanocrystals

Acne is a common inflammatory skin disease which affects the hair follicles of the skin.[12] Some inflammatory factors, such as TNF- α and IL-6, play a key role in the pathogenesis of inflammatory diseases and reflect the degree of inflammation.[53] In this part of the experiment, the inflammatory evaluation model of macrophages induced by LPS was constructed. Cell viability was determined using an MTT assay. As shown in Figure 6A-D, none of the test groups at a concentration of 0.2% (w/w) showed obvious toxicity to RAW 264.7 cells. It was reported that dexamethasone had no macrophage toxicity at the concentration of 0.2%.[54] Consequently, the concentration of 0.2% was selected for further

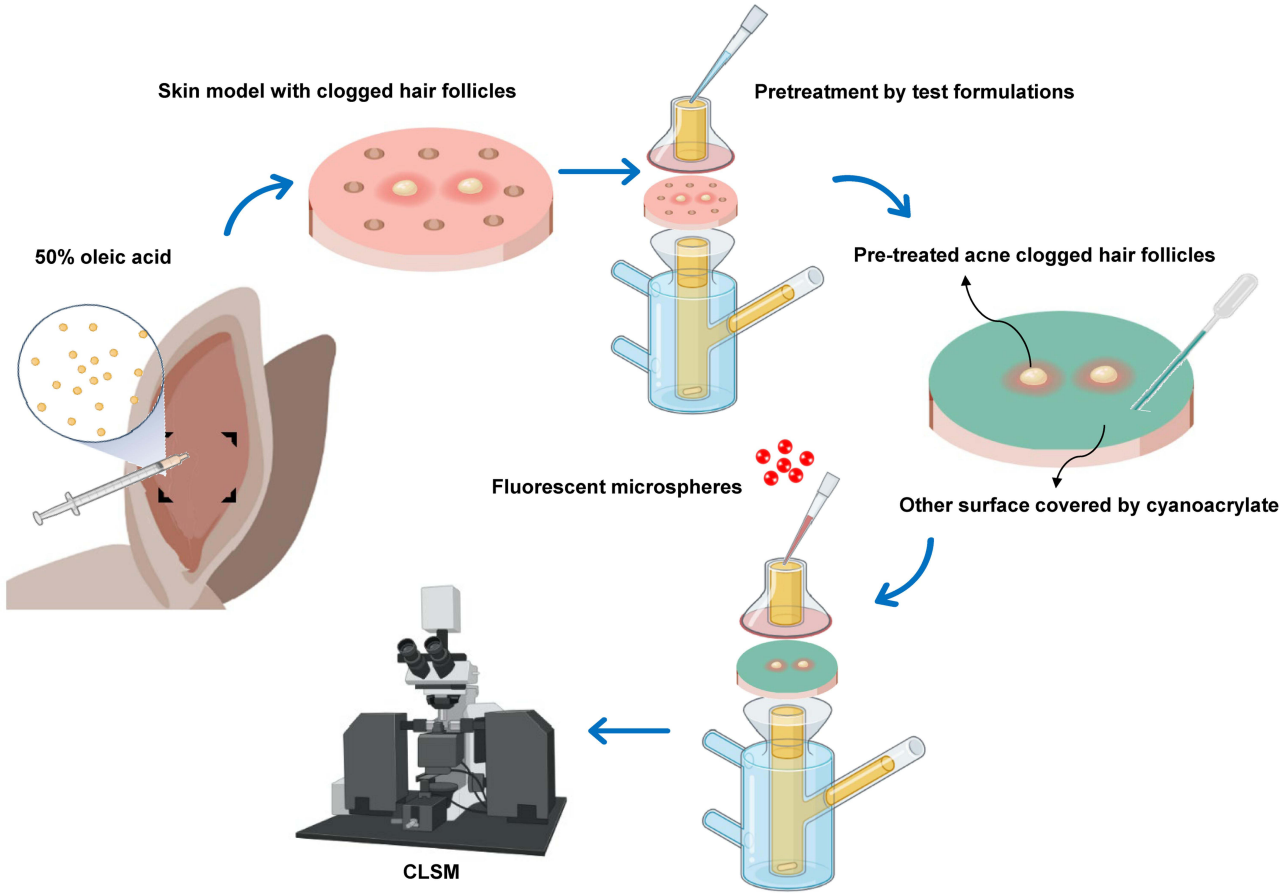

Figure 4 Diagrammatic sketch of the experiment of penetrating into clogged hair follicles.

anti-inflammatory experiments. The anti-inflammatory effects of different solution were evaluated on LPS treated RAW 264.7 macrophages by determination of inflammatory factor level. As shown in Figure 6E and F, the levels of TNF-α and IL-6 in the LPS induction group were higher than those in the unstimulated blank group, and the levels of TNF-α and IL-6 in the DEX group were significantly lower than those in the LPS induction group, suggesting that the LPS-induced inflammatory cell model was effectively constructed. The levels of IL-6 secretion in each experimental group were as follows: AZA group < DEX group < Piper methysticum extract group < D. candidum extract group < A. barbadensis extract group. The levels of TNF-α secretion in each experimental group were as follows: DEX group < AZA micro/nanocrystal group < Piper methysticum extract group < Dendrobium candidum extract group < A. barbadensis extract group. The levels of TNF-α and IL-6 in the DEX and AZA micro/nanocrystal groups significantly decreased. These results suggested that AZA micro/nanocrystals can inhibit the secretion of the inflammatory factors TNF-α and IL-6 and effectively reduce inflammation. This was because AZA possessed a direct anti-inflammatory effect owing to its free oxygen radical-scavenging activity.[55]

In vitro Antibacterial Effect of AZA Micro/Nanocrystals

The inhibitory effects of different test solutions on the growth of Cutibacterium acnes are shown in Table 3. The MIC of AZA micro/nanocrystals on Cutibacterium acnes was 0.1%, which was the lowest among all the experimental groups. The order of MIC in the different experimental groups from low to high was AZA micro/nanocrystals, Pionin, and P. granatum, with MIC values of 0.1%, 0.15%, and 0.25%, respectively. The MIC of R. roosea was not found at the experimental concentrations and may be higher than 0.25%.

As illustrated in Figure 7, different test solutions showed different inhibitory effects on the growth of Cutibacterium acnes. For example, the inhibitory rates at a concentration of 0.1% were in the order of Rhodiola

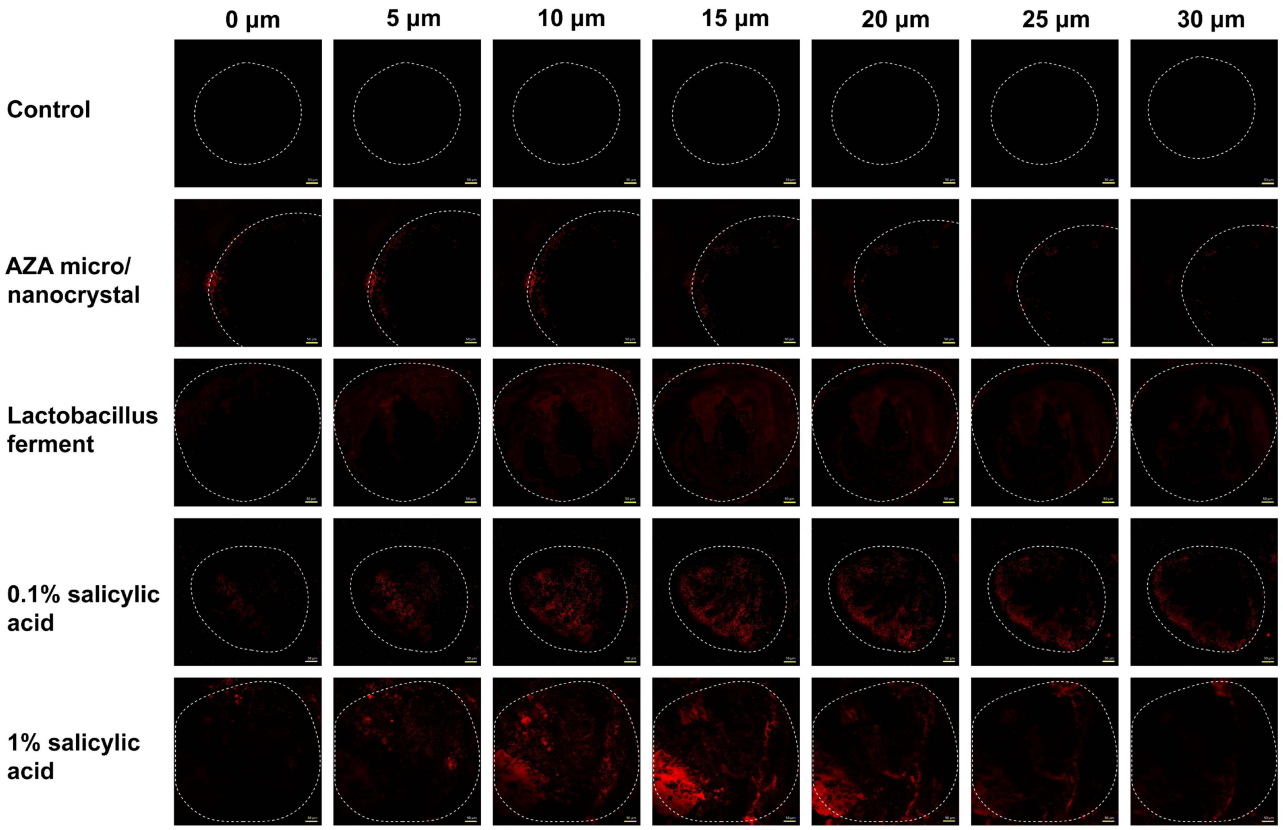

Figure 5 Fluorescence microscopic images in different skin depths, scale bar 50 μm.

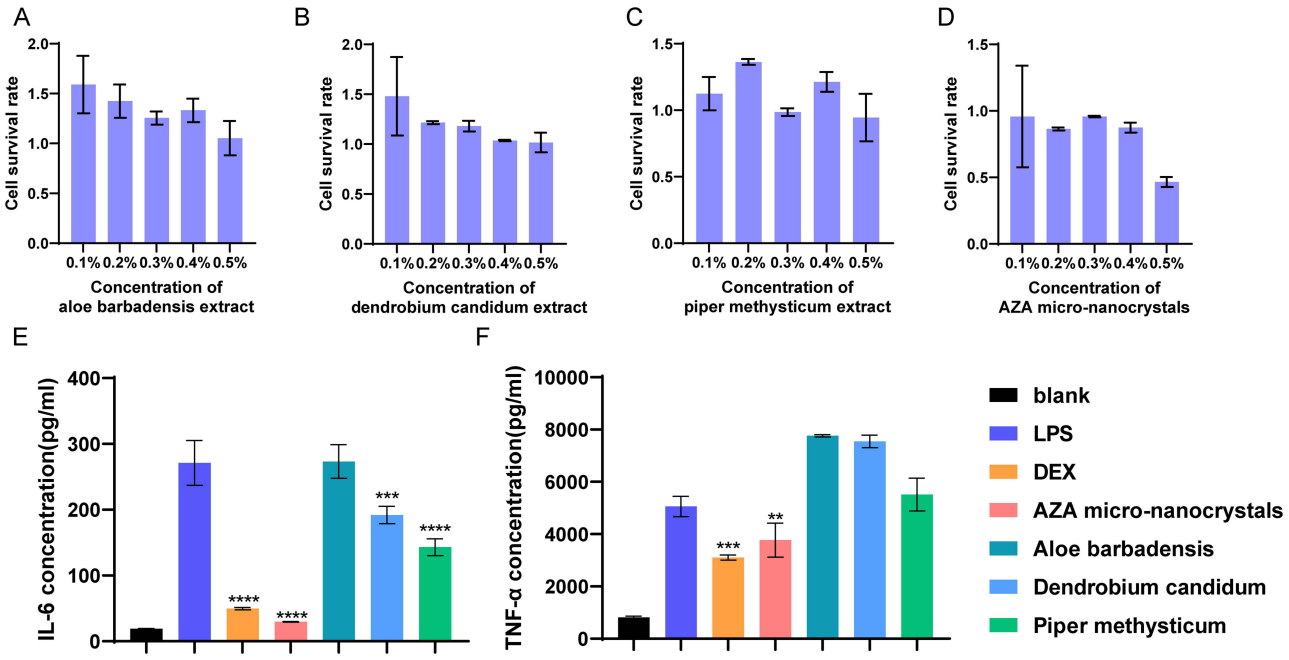

Figure 6 Cell viability of the in vitro cytotoxicity studies in RAW 264.7 (**A-D**). IL-6 and TNF- α concentration in the collected supernatants secreted by RAW 264.7 cells after treating with LPS, DEX, AZA, other extracts and normal medium, respectively (**E** and **F**). **p < 0.01, ***p < 0.001, ****p < 0.0001 (n=3, mean ± SD). DEX: dexamethasone; LPS, Lipopolysaccharide.

Table 3 Visible Growth of Cutibacterium Acnes in Different Experimental Groups (n=3)

Concentration of Test Solution	Test Solution			
	AZA micro/ Nanocrystals	Pionin	Punica Granatum	Rhodiola Rosea
0.25%	–	–	–	+
0.2%	–	–	+	+
0.15%	–	–	+	+
0.1%	–	+	+	+
0.05%	+	+	+	+

Notes: +: visible growth was observed; -: no visible growth was observed.

rosea extract group < Pionin group < P. granatum extract group <AZA micro/nanocrystals group. Among these groups, AZA exhibited the best inhibitory effects against Cutibacterium acnes at all concentrations, which was consistent with the MIC results. The antibacterial effects of AZA may be linked to a decrease in bacterial intracellular pH, disruption of the maintenance of a pH gradient along the cell membrane, and induction of widespread energy loss in bacterial metabolism. This mechanism of action also diminishes the possibility of bacteria developing resistance to AZA.[55]

Comparison of Skin Irritation Between AZA Micro/Nanocrystals and Commercial Products

As shown in Figure 8, similar to the control group (group A), the optimized AZA micro/nanocrystals containing 1% salicylic acid with ultrasound exposure (group C) did not produce irritant reactions such as erythema and edema (irritation score = 0). However, the AZA commercial product (group D) produced mild erythema with an irritation score of 0.25±0.50. The positive control (group B) showed more severe erythema, with an irritation score of 2.75±0.50. The results showed that the optimized AZA micro/nanocrystals achieved satisfactory skin safety compared with the AZA commercial product, which exhibited the advantage of hair follicle-targeted delivery for skin safety. It was worth noting that salicylic acid was reported to have the potential for skin irritation,[56,57] slow-released salicylic acid was selected in this work, encapsulated by hydroxypropyl cyclodextrin, which did not produce clear irritant reactions according to the above results.

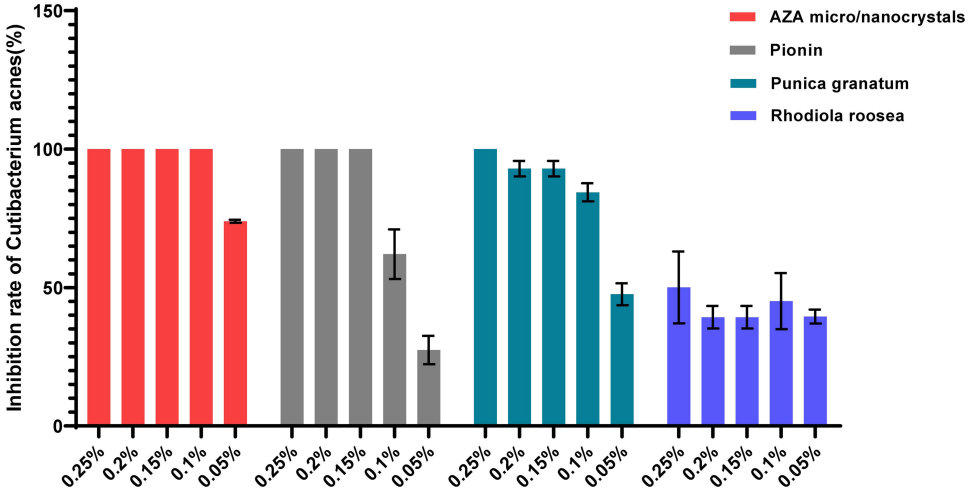

Figure 7 Inhibitory rate of different test solution on Cutibacterium acnes (n=3, mean ± SD).

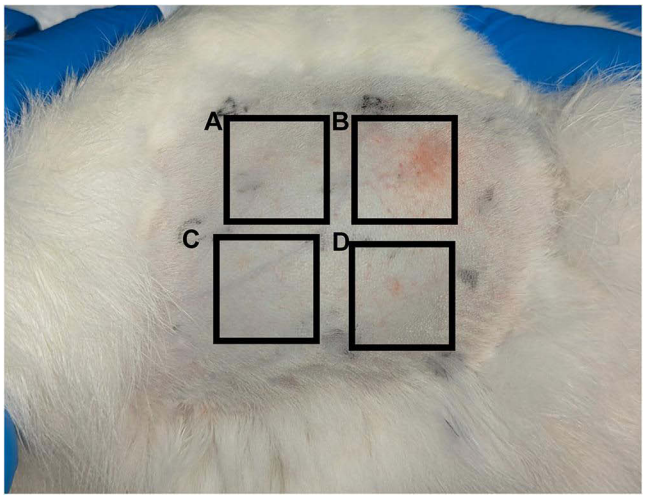

Figure 8 The skin irritation test with five rabbits per group. The skin situation in the control group (**A**), 5% SDS group (**B**), 10% AZA micro/nanocrystals containing 1% salicylic acid with ultrasound (**C**), 10% commercial AZA gel (**D**) (n = 5).

In vivo Therapeutic Effect of AZA Micro/Nanocrystals on Acne

As shown in Figure 9A, a composite acne model was constructed and induced by intradermal injection of Cutibacterium acnes and topical application of 30% oleic acid. Compared with the clogged hair follicle model described in Section 3.3.1, this composite acne model involving Cutibacterium acnes was more consistent with the pathological process of acne,[58] and thus, was employed to evaluate the therapeutic effect on acne in vivo. As shown in the control group in Figures 9B and 10, the constructed acne was characterized by dilatation, blockage, and hyperkeratosis of the hair follicle with a red protuberance observed by a digital camera and a dermatoscope. The skin of the rabbit ear was rougher and thicker than that of the healthy skin. H&E staining and Oil Red O staining (Figure 11) showed dense inflammatory infiltration at the site of acne, and hyperkeratosis, epidermal thickening, and destruction of sebaceous glands were found in comparison to healthy skin. The above observation results for the constructed composite acne model were consistent with the reported characteristics of acne,[59] showing that the composite acne model was successfully established.

As shown in Figure 9B, the epidermis remained intact in all groups. Both treatment groups showed improvement without adverse effects compared with the control group. Compared with the commercial group, the red bulge of acne was significantly diminished in the experimental group (Figure 9B). Figure 10 shows an identical result with a dermatoscope, which could provide clearer photos (Figure 10A) and a quantitative description (Figures 10B and C) of the acne morphology. Compared with the other groups, the experimental group showed an obvious decrease in acne diameter, which was approximately twice that of the commercial group (Figure 10B). In addition, the experimental group had the smallest pixel difference in color intensity between the acne area and surrounding skin area. The pixel difference in the commercial group was more than twice that of the experimental group (Figure 10C). In the H&E staining results (Figure 11), compared to the commercial group, the acne bulge was obviously diminished in the experimental group. Moreover, there was a clear reduction in the inflammatory infiltration at the acne site in the experimental group. Both H&E and Oil Red O staining results showed that there was a recovery of the thickness of the epidermis to a healthy state in the experimental group, while the thickness of the epidermis in the commercial group was almost unchanged. The above results indicated that AZA micro/nanocrystals exhibited an advantage over commercial products in terms of the therapeutic effect on acne, which was attributed to their ability of hair follicle-targeted delivery as well as their excellent anti-inflammatory and antibacterial effects.

In this work, rabbit ear follicles were employed as an animal model, since they were similar to human follicles in that both possessed small pili and large adjacent sebaceous glands.[60] Also, rabbit ear follicles were sensitive to the degree that only two weeks of applying a test agent can produce erythema, desquamation, and follicular keratosis, making the model useful for in vivo efficacy experiment. However, established acne lesions cannot be maintained for more than five days

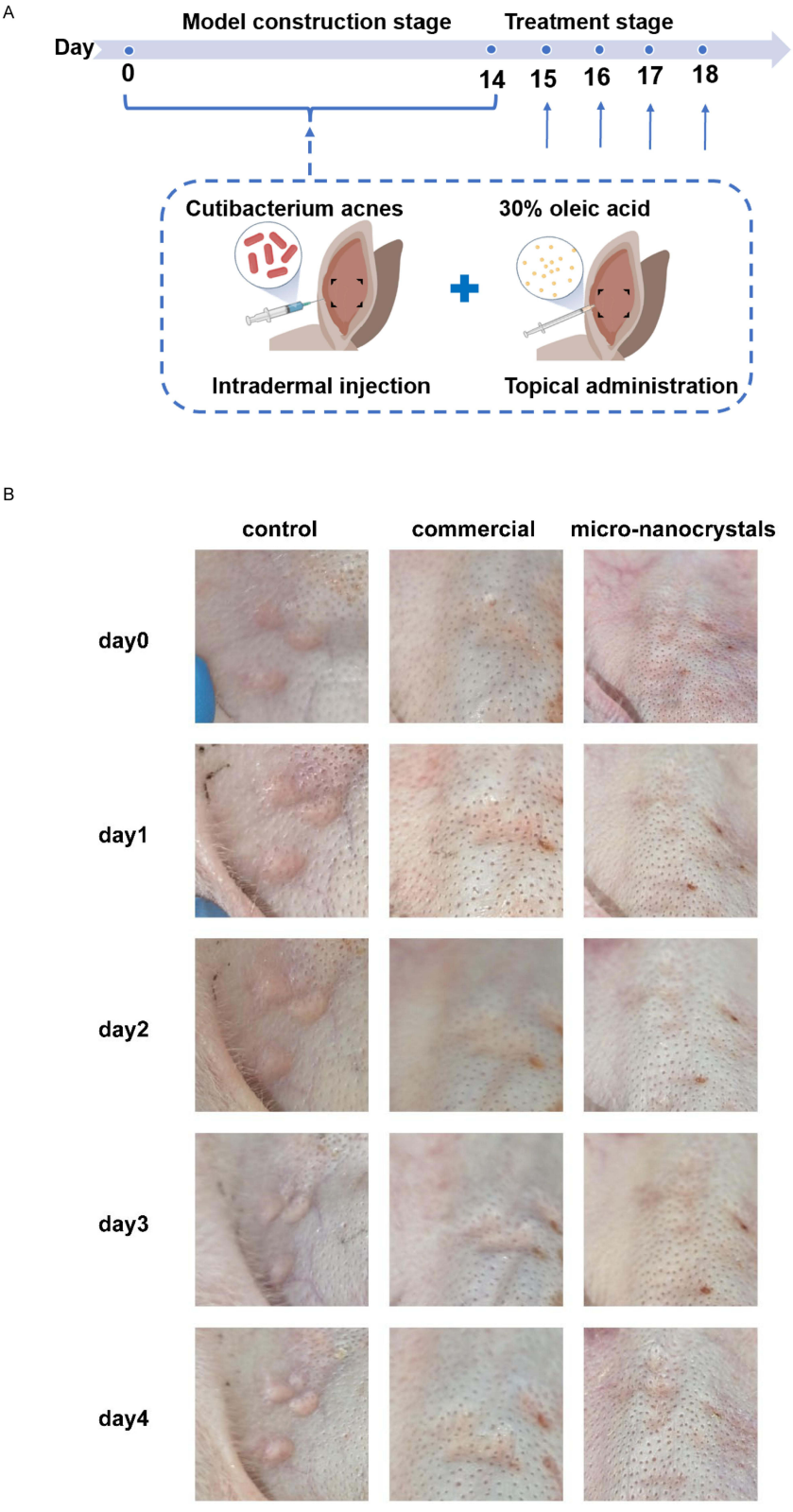

Figure 9 (**A**) Construction method of composite acne model and treatment regimen, (**B**) Changes observed by digital camera during acne treatment (n = 5).

https://doi.org/10.2147/IJN.S459788 DovePress

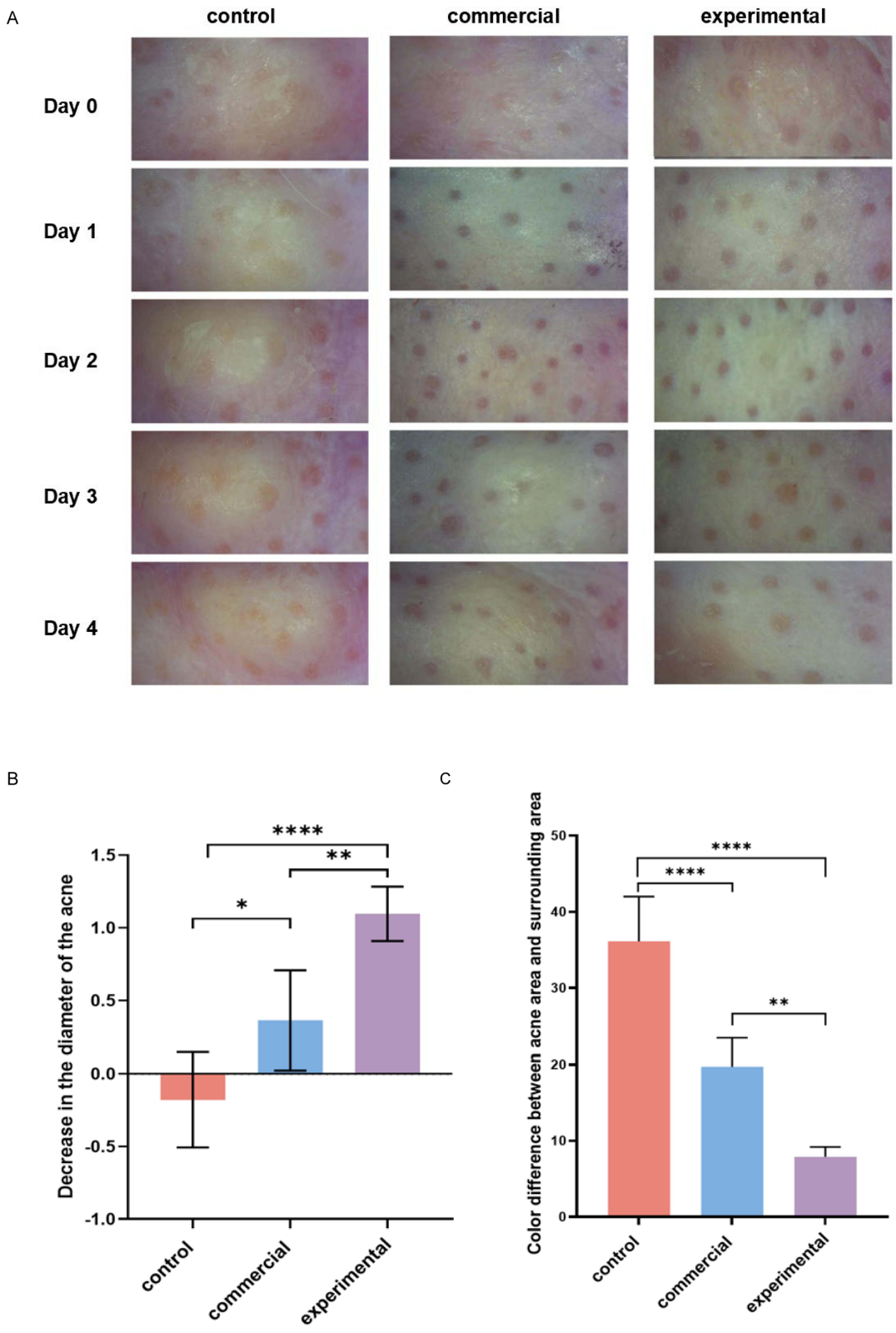

Figure 10 (**A**) Dermatoscope observation in acne composite model after treatment, (**B**) Decrease in the diameter of the acne between day 0 and day 4 after treatment, (**C**) Color differences between acne and its surrounding skin in day 4 after treatment. *p < 0.05, **p < 0.01, ****p < 0.0001 (n = 5, mean ± SD).

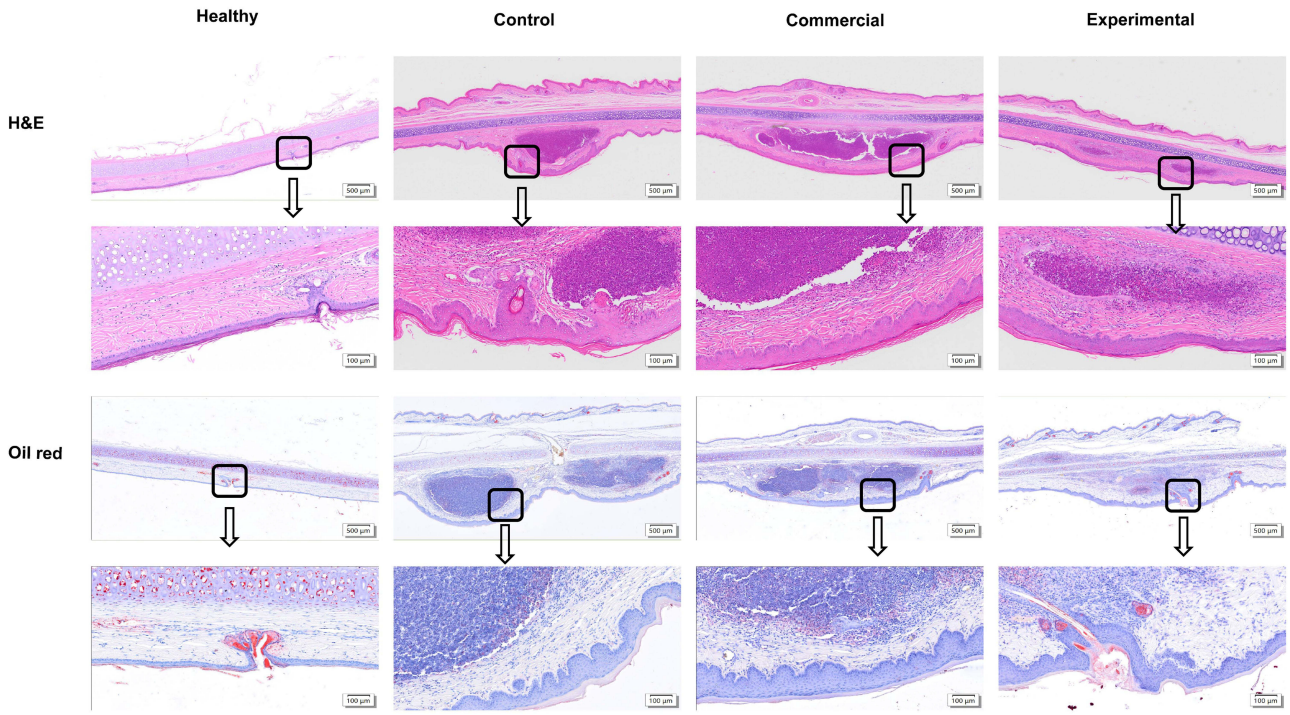

Figure 11 Histopathological analysis of acne composite model at the fourth day after treatment. Scale bar 500 μm (upper) and100 μm (lower).

because of the limited extent of bacterial colonization.[60] Therefore, rabbit ear follicles were limited in that they can only be used to observe the short-term effectiveness of acne treatment.

Conclusion

AZA micro/nanocrystals exhibited the ability to target hair follicles compared with commercial products. Targeting ability was remarkably enhanced when combined with ultrasound exposure. Toward the clogged hair follicles, AZA micro/nanocrystals cannot easily penetrate by themselves. Only with the help of the 1% salicylic acid, AZA micro/nanocrystals had great potential for penetrating clogged hair follicles. AZA micro/nanocrystals had anti-inflammatory effects, inhibiting the levels of pro-inflammatory factors, and antibacterial effects on the growth of Cutibacterium acnes. Compared with commercial products, the combination of AZA micro/nanocrystals and ultrasound exhibited an obvious advantage in terms of both skin safety and in vivo anti-acne therapeutic efficacy. In conclusion, hair follicle-targeted delivery of AZA micro/nanocrystals provided a satisfactory alternative in promoting the treatment of acne vulgaris.

Abbreviations

AZA, azelaic acid; DEX, dexamethasone; LPS, Lipopolysaccharide.

Acknowledgments

This work was financially supported by the National Natural Science Foundation of China (No. 82374049) and “Double First-Class” University Project (CPU2022QZ09).

Disclosure

The authors report a patent CN116747147A pending, grants from Nanjing Miaobang Meiye Enterprise Management Co., Ltd. during the conduct of the study. The authors declare that they have no other conflicts of interest in this work.

References

1. Patel R, Prabhu P. Nanocarriers as versatile delivery systems for effective management of acne. *Int J Pharm*. 2020;579.
2. Tuchayi SM, Makrantonaki E, Ganceviciene R, Dessinioti C, Feldman SR, Zouboulis CC. Acne vulgaris. *Nature Reviews Disease Primers*. 2015;1 (1):548.
3. Gollnick HP, Zouboulis CC. Not all acne is acne vulgaris. *Dtsch Arztebl Int*. 2014;111(17):301–312. doi:10.3238/arztebl.2014.0301
4. Dreno B, Bagatin E, Blume-Peytavi U, Rocha M, Gollnick H. Female type of adult acne: physiological and psychological considerations and management. *J Dtsch Dermatol Ges*. 2018;16(10):1185–1194.
5. Aslan Kayiran M, Karadag AS, Jafferany M. Psychodermatology of acne: dermatologist's guide to inner side of acne and management approach. *Dermatol Ther*. 2020;33(6):e14150. doi:10.1111/dth.14150
6. Revol O, Milliez N, Gerard D. Psychological impact of acne on 21st-century adolescents: decoding for better care. *Br J Dermatol*. 2015;172 Suppl 1:52–58. doi:10.1111/bjd.13749
7. Nast A, Dréno B, Bettoli V, et al. European evidence-based (S3) guideline for the treatment of acne – update 2016 – short version. *J Eur Acad Dermatol Venereol*. 2016;30(8):1261–1268. doi:10.1111/jdv.13776
8. Paiva-Santos AC, Mascarenhas-Melo F, Coimbra SC, et al. Nanotechnology-based formulations toward the improved topical delivery of anti-acne active ingredients. *Expert Opin Drug Deliv*. 2021;18(10):1435–1454. doi:10.1080/17425247.2021.1951218
9. Tang SC, Yang JH. Dual Effects of Alpha-Hydroxy Acids on the Skin. *Molecules*. 2018;23(4):863. doi:10.3390/molecules23040863
10. Kosmadaki M, Katsambas A. Topical treatments for acne. *Clin Dermatol*. 2017;35(2):173–178. doi:10.1016/j.clindermatol.2016.10.010
11. Habeshian KA, Cohen BA. Current Issues in the Treatment of Acne Vulgaris. *Pediatrics*. 2020;145(Supplement_2):S225–S230. doi:10.1542/peds.2019-2056L
12. Dréno B. What is new in the pathophysiology of acne, an overview. *J Eur Acad Dermatol Venereol*. 2017;31(Suppl 5):8–12. doi:10.1111/jdv.14374
13. Bhate K, Williams HC. Epidemiology of acne vulgaris. *Br J Dermatol*. 2013;168(3):474–485. doi:10.1111/bjd.12149
14. Zouboulis CC, Jourdan E, Picardo M. Acne is an inflammatory disease and alterations of sebum composition initiate acne lesions. *J Eur Acad Dermatol Venereol*. 2013;28(5):527–532. doi:10.1111/jdv.12298
15. Sommatis S, Capillo MC, Maccario C, et al. Biophysical and Biological Tools to Better Characterize the Stability, Safety and Efficacy of a Cosmeceutical for Acne-Prone Skin. *Molecules*. 2022;27(4):1255. doi:10.3390/molecules27041255
16. Parmar PK, Wadhawan J, Bansal AK. Pharmaceutical nanocrystals: a promising approach for improved topical drug delivery. *Drug Discovery Today*. 2021;26(10):2329–2349. doi:10.1016/j.drudis.2021.07.010
17. Cui M, Wiraja C, Chew SWT, Xu C. Nanodelivery Systems for Topical Management of Skin Disorders. *Mol Pharmaceut*. 2021;18(2):491–505. doi:10.1021/acs.molpharmaceut.0c00154
18. Chutoprapat R, Kopongpanich P, Chan LW. A Mini-Review on Solid Lipid Nanoparticles and Nanostructured Lipid Carriers: topical Delivery of Phytochemicals for the Treatment of Acne Vulgaris. *Molecules*. 2022;27(11):3460. doi:10.3390/molecules27113460
19. Eroğlu C, Sinani G, Ulker Z. Current State of Lipid Nanoparticles (SLN and NLC) for Skin Applications. *Curr. Pharm. Des*. 2023;29 (21):1632–1644. doi:10.2174/1381612829666230803111120
20. Alvi SB, Rajalakshmi PS, Jogdand A, et al. Iontophoresis mediated localized delivery of liposomal gold nanoparticles for photothermal and photodynamic therapy of acne. *Biomater. Sci*. 2021;9(4):1421–1430. doi:10.1039/D0BM01712D
21. Xiang Y, Lu J, Mao C, et al. Ultrasound-triggered interfacial engineering-based microneedle for bacterial infection acne treatment. *Sci Adv*. 2023;9 (10):eadf0854. doi:10.1126/sciadv.adf0854
22. Rapalli VK, Kaul V, Waghule T, et al. Curcumin loaded nanostructured lipid carriers for enhanced skin retained topical delivery: optimization, scale-up, in-vitro characterization and assessment of ex-vivo skin deposition. *Eur j Pharmaceutical Sci*. 2020;152:105438. doi:10.1016/j.ejps.2020.105438
23. Ahmad Nasrollahi S, Koohestani F, Naeimifar A, Samadi A, Vatanara A, Firooz A. Preparation and evaluation of Adapalene nanostructured lipid carriers for targeted drug delivery in acne. *Dermatol Ther*. 2021;34(2):e14777. doi:10.1111/dth.14777
24. Liu Y, Zhao J, Chen J, Miao X. Nanocrystals in cosmetics and cosmeceuticals by topical delivery. *Colloids Surf. B*. 2023;227:113385. doi:10.1016/j.colsurfb.2023.113385
25. Raszewska-Famielec M, Flieger J. Nanoparticles for Topical Application in the Treatment of Skin Dysfunctions-An Overview of Dermo-Cosmetic and Dermatological Products. *Int J Mol Sci*. 2022;23(24). doi:10.3390/ijms232415980
26. Patzelt A, Lademann J. Recent advances in follicular drug delivery of nanoparticles. *Expert Opin Drug Deliv*. 2020;17(1):49–60. doi:10.1080/17425247.2020.1700226
27. Yazdani-Arazi SN, Ghanbarzadeh S, Adibkia K, Kouhsoltani M, Hamishehkar H. Histological evaluation of follicular delivery of arginine via nanostructured lipid carriers: a novel potential approach for the treatment of alopecia. *Artif. Cells Nanomed. Biotechnol*. 2017;45(7):1379–1387. doi:10.1080/21691401.2016.1241794
28. Friedman N, Dagan A, Elia J, Merims S, Benny O. Physical properties of gold nanoparticles affect skin penetration via hair follicles. *Nanomedicine*. 2021;36:102414. doi:10.1016/j.nano.2021.102414
29. Ushirobira CY, Afiune LAF, Pereira MN, Cunha-Filho M, Gelfuso GM, Gratieri T. Dutasteride nanocapsules for hair follicle targeting: effect of chitosan-coating and physical stimulus. *Int J Biol Macromol*. 2020;151:56–61. doi:10.1016/j.ijbiomac.2020.02.143
30. Tomić I, Miočić S, Pepić I, Šimić D, Filipović-Grčić J. Efficacy and Safety of Azelaic Acid Nanocrystal-Loaded In Situ Hydrogel in the Treatment of Acne Vulgaris. *Pharmaceutics*. 2021;13(4):567. doi:10.3390/pharmaceutics13040567
31. Tang X, Liu Y, Yuan H, Gao R. Development of a Self-Assembled Hydrogels Based on Carboxymethyl Chitosan and Oxidized Hyaluronic Acid Containing Tanshinone Extract Nanocrystals for Enhanced Dissolution and Acne Treatment. *Pharmaceuticals*. 2022;15(12):1534. doi:10.3390/ph15121534
32. Folle C, Díaz-Garrido N, Sánchez-López E, et al. Surface-Modified Multifunctional Thymol-Loaded Biodegradable Nanoparticles for Topical Acne Treatment. *Pharmaceutics*. 2021;13(9):1501. doi:10.3390/pharmaceutics13091501
33. Kumar V, Banga AK. Intradermal and follicular delivery of Adapalene liposomes. *Drug Dev Ind Pharm*. 2016;42(6):871–879. doi:10.3109/03639045.2015.1082580

34. Ferreira-Nunes R, Cunha-Filho M, Gratieri T, Gelfuso GM. Follicular-targeted delivery of spironolactone provided by polymeric nanoparticles. *Colloids and Surfaces B: Biointerfaces*. 2021;208:112101. doi:10.1016/j.colsurfb.2021.112101
35. Mohammad IS, Hu H, Yin L, He W. Drug nanocrystals: fabrication methods and promising therapeutic applications. *Int J Pharm*. 2019;562:187–202. doi:10.1016/j.ijpharm.2019.02.045
36. Hughes AJ, Tawfik SS, Baruah KP. Tape strips in dermatology research. *Br J Dermatol*. 2021;185(1):26–35. doi:10.1111/bjd.19760
37. Al Mahrooqi JH, Khutoryanskiy VV, Williams AC. Thiolated and PEGylated silica nanoparticle delivery to hair follicles. *Int J Pharm*. 2021;593:120130. doi:10.1016/j.ijpharm.2020.120130
38. Tolentino S, Pereira MN, Cunha-Filho M, Gratieri T, Gelfuso GM. Targeted clindamycin delivery to pilosebaceous units by chitosan or hyaluronic acid nanoparticles for improved topical treatment of acne vulgaris. *Carbohydr Polym*. 2021;253:117295. doi:10.1016/j.carbpol.2020.117295
39. Kumar V, Banga AK. Intradermal and follicular delivery of Adapalene. *Drug Dev. Ind. Pharm.* 2015;42(6):871–879.
40. Yang J, Geng Q, Zhou Y, Wang Y, Li Z, Liu Y. Optimization of Experimental Procedure for Determining Azelaic Acid in Cosmetics by Gas Chromatography Derivatized through Ethanol. *ACS omega*. 2022;7(18):15647–15656. doi:10.1021/acsomega.2c00464
41. Facchin BM, Dos Reis GO, Vieira GN, et al. Inflammatory biomarkers on an LPS-induced RAW 264.7 cell model: a systematic review and meta-analysis. *Inflammation Res*. 2022;71(7–8):741–758. doi:10.1007/s00011-022-01584-0
42. Wu J, Guo R, Chai J, et al. The Protective Effects of Cath-MH With Anti-Propionibacterium Acnes and Anti-Inflammation Functions on Acne Vulgaris. *Front Pharmacol*. 2021;12:788358. doi:10.3389/fphar.2021.788358
43. Qin Z, Chen F, Chen D, Wang Y, Tan Y, Ban J. Transdermal permeability of triamcinolone acetonide lipid nanoparticles. *Int J Nanomed*. 2019;14:2485–2495. doi:10.2147/IJN.S195769
44. Gu Y, Bian Q, Zhou Y, Huang Q, Gao J. Hair follicle-targeting drug delivery strategies for the management of hair follicle-associated disorders. *Asian J. Pharm. Sci.* 2022;17(3):333–352. doi:10.1016/j.ajps.2022.04.003
45. Paithankar D, Hwang BH, Munavalli G, et al. Ultrasonic delivery of silica–gold nanoshells for photothermolysis of sebaceous glands in humans: nanotechnology from the bench to clinic. *J Control Release*. 2015;206:30–36. doi:10.1016/j.jconrel.2015.03.004
46. Fox L, Csongradi C, Aucamp M, du Plessis J, Gerber M. Treatment Modalities for Acne. *Molecules*. 2016;21(8):1063. doi:10.3390/molecules21081063
47. Kandekar SG, Del Río-Sancho S, Lapteva M, Kalia YN. Selective delivery of Adapalene to the human hair follicle under finite dose conditions using polymeric micelle nanocarriers. *Nanoscale*. 2018;10(3):1099–1110. doi:10.1039/C7NR07706H
48. Patzelt A, Richter H, Knorr F, et al. Selective follicular targeting by modification of the particle sizes. *J Control Release*. 2011;150(1):45–48. doi:10.1016/j.jconrel.2010.11.015
49. Horita D, Yoshimoto M, Todo H, Sugibayashi K. Analysis of hair follicle penetration of lidocaine and fluorescein isothiocyanate-dextran 4 kDa using hair follicle-plugging method. *Drug Dev Ind Pharm*. 2014;40(3):345–351. doi:10.3109/03639045.2012.762653
50. Chandrasekaran NC, Sanchez WY, Mohammed YH, Grice JE, Roberts MS, Barnard RT. Permeation of topically applied Magnesium ions through human skin is facilitated by hair follicles. *Magnesium Res*. 2016;29(2):35–42. doi:10.1684/mrh.2016.0402
51. Abdel Meguid AM, Ahmed Attallah DA E, Omar H. Trichloroacetic Acid Versus Salicylic Acid in the Treatment of Acne Vulgaris in Dark-Skinned Patients. *Dermatologic Surg*. 2015;41(12):1398–1404. doi:10.1097/DSS.0000000000000522
52. Bisht A, Hemrajani C, Upadhyay N, et al. Azelaic acid and Melaleuca alternifolia essential oil co-loaded vesicular carrier for combinational therapy of acne. *Therapeutic Delivery*. 2022;13(1):13–29. doi:10.4155/tde-2021-0059
53. Yang CL, Wu HC, Hwang TL, et al. Anti-Inflammatory and Antibacterial Activity Constituents from the Stem of Cinnamomum validinerve. *Molecules*. 2020;25(15):3382. doi:10.3390/molecules25153382
54. Zhou M, Tang Y, Liao L, et al. Phillygenin inhibited LPS-induced RAW 264.7 cell inflammation by NF-κB pathway. *Eur. J. Pharmacol.* 2021;899:174043. doi:10.1016/j.ejphar.2021.174043
55. Sieber MA, Hegel JKE. Azelaic Acid: properties and Mode of Action. *Skin Pharmacol Physiol*. 2014;27(Suppl. 1):9–17. doi:10.1159/000354888
56. Draelos ZD. The Efficacy and Tolerability of Turmeric and Salicylic Acid in Psoriasis Treatment. *Psoriasis*. 2022;12:63–71.
57. Lee KC, Wambier CG, Soon SL, et al. Basic chemical peeling: superficial and medium-depth peels. *J Am Acad Dermatol*. 2019;81(2):313–324. doi:10.1016/j.jaad.2018.10.079
58. Dréno B, Pécastaings S, Corvec S, Veraldi S, Khammari A, Roques C. Cutibacterium acnes (Propionibacterium acnes) and acne vulgaris: a brief look at the latest updates. *J Eur Acad Dermatol Venereol*. 2018;32 Suppl 2:5–14. doi:10.1111/jdv.15043
59. Williams HC, Dellavalle RP, Garner S. Acne vulgaris. *Lancet*. 2012;379(9813):361–372. doi:10.1016/S0140-6736(11)60321-8
60. Seok J, Kim JH, Kim JM, et al. Effects of Intradermal Radiofrequency Treatment and Intense Pulsed Light Therapy in an Acne-induced Rabbit Ear Model. *Sci Rep*. 2019;9(1). doi:10.1038/s41598-019-41322-x